

# Kinetics of Shear Induced Structural Ordering in Dense Colloids

HongRui He,<sup>†,§</sup> Jonghun Lee,<sup>‡</sup> Zhang Jiang,<sup>‡</sup> Qiming He,<sup>†,§</sup> Jelena Dinic,<sup>†,§</sup> Wei  
Chen,<sup>†,§</sup> Suresh Narayanan,<sup>\*,‡</sup> and Xiao-Min Lin<sup>\*,¶</sup>

<sup>†</sup>*Materials Science Division and Center for Molecular Engineering, Argonne National  
Laboratory, Argonne, IL 60439*

<sup>‡</sup>*X-ray Science Division, Advanced Photon Source, Argonne National Laboratory, Argonne,  
IL 60439*

<sup>¶</sup>*Center for Nanoscale Materials, Argonne National Laboratory, Argonne, IL 60439*

<sup>§</sup>*Pritzker School of Molecular Engineering, University of Chicago, Chicago, IL 60637*

E-mail: sureshn@anl.gov; xmlin@anl.gov

## Abstract

The macroscopic rheological response of a colloidal solution is highly correlated with the local microscopic structure, as revealed by an *in situ* Rheo-SAXS experiment with a high temporal resolution. Oscillatory shear can induce a strain-controlled ordering-to-disorder transition, resulting in a shear thickening process that is different from the normal shear thickening behavior that is driven by hydrodynamics and particle friction. We reveal that there is a complex time-dependent kinetics towards structural ordering under different applied strains. When the strain amplitude reaches a critical value that starts to induce disordering in the system, the pathway towards the dynamic equilibrium can also become highly non-monotonic. Within the same oscillatory cycle, there is a strong correlation of ordering with different phase of the oscillation, with the system oscillating between two dynamic metastable states.

## 1 Introduction

Complex fluids made of Brownian nanoparticles are ubiquitous in nature as well as in many man-made products. Their rheological response exhibits some unique behaviors that are closely related to their internal structure.<sup>1</sup> The classical nucleation theory under equilibrium condition predicts that, when the particle concentration reaches a certain critical value, the density fluctuation first triggers the formation of small nuclei. Beyond a critical size, these nuclei would spontaneously grow driven by the entropy of the system and particle interactions.<sup>2</sup> For hard spheres, both theories and experiments confirmed a crystal-liquid coexistence region with volume fraction  $\phi$  in the range of  $0.494 < \phi < 0.545$ , a crystal region  $0.545 < \phi < 0.57$ , and a glassy region when  $\phi > 0.57$ .<sup>3</sup> However, these thermodynamically favored states may not be observed directly in experiment, simply because the system might be trapped in many metastable states when the kinetics driving the system towards equilibrium is slower than the experimental time. In many cases, an external stimulant, such as a shear force, can be applied to speed up the kinetics towards equilibrium. Shear induced

structural formation, however, is a highly non-equilibrium process and may be influenced by other parameters, such as the type of shear applied, shear rate, shear duration, volume fraction and residue structures in the quiescent state. Different shear rates can either suppress or promote crystallization.<sup>4</sup> It is well known that an intermediate shear rate in a complex fluid can induce structural ordering of its constituent particles. Experimental work in this area date back to several decades ago by Hoffman,<sup>5</sup> Ackerson and Pusey,<sup>6</sup> Clark et al.,<sup>7</sup> Haw et al.<sup>8</sup> Theoretical simulations are based primarily on Stokesian dynamics, which have reproduced some of the ordered structures, but some of these results are inconsistent with the structure observed under similar experimental conditions.<sup>9,10</sup> A recent work by Xu et al. indicated that replacing a periodic boundary condition with a planar boundary condition in simulation actually yield ordered structures much closer to experimental data.<sup>11</sup>

More recently, studies in the this area have been driven by the need to understand more deeply the relationship between the structural ordering and the rheological behavior of colloids, in particularly with regard to shear thinning and shear thickening behavior.<sup>11-15</sup> It is well known that flow induced crystals at low shear rate can undergo an order-to-disorder transition driven by hydrodynamic interactions between the particles. Hoffman proposed that this type of transition is responsible for shear thickening, i.e. a large increase of viscosity beyond certain critical shear stress.<sup>5,16</sup> However, not all colloids showing shear thickening behavior have demonstrated order-to-disorder transition, thus the relationship between shear induced order-to-disorder transition and shear thickening remained somewhat ambiguous.<sup>17</sup> In our previous study, we have shown that, for a monodispersed colloid, oscillatory shear can induce an order-to-disorder transition that is well-separated from the critical stress for normal shear thickening.<sup>12</sup> Particle size, monodispersity and oscillatory frequency all play a role in the separation of order-to-disorder transition with normal shear thickening. This two-step shear thinning and thickening clearly show that an order-to-disorder transition is different in mechanism than the one inducing shear thickening.

Understanding the kinetics of crystallization under shear flow, the stability of ordered

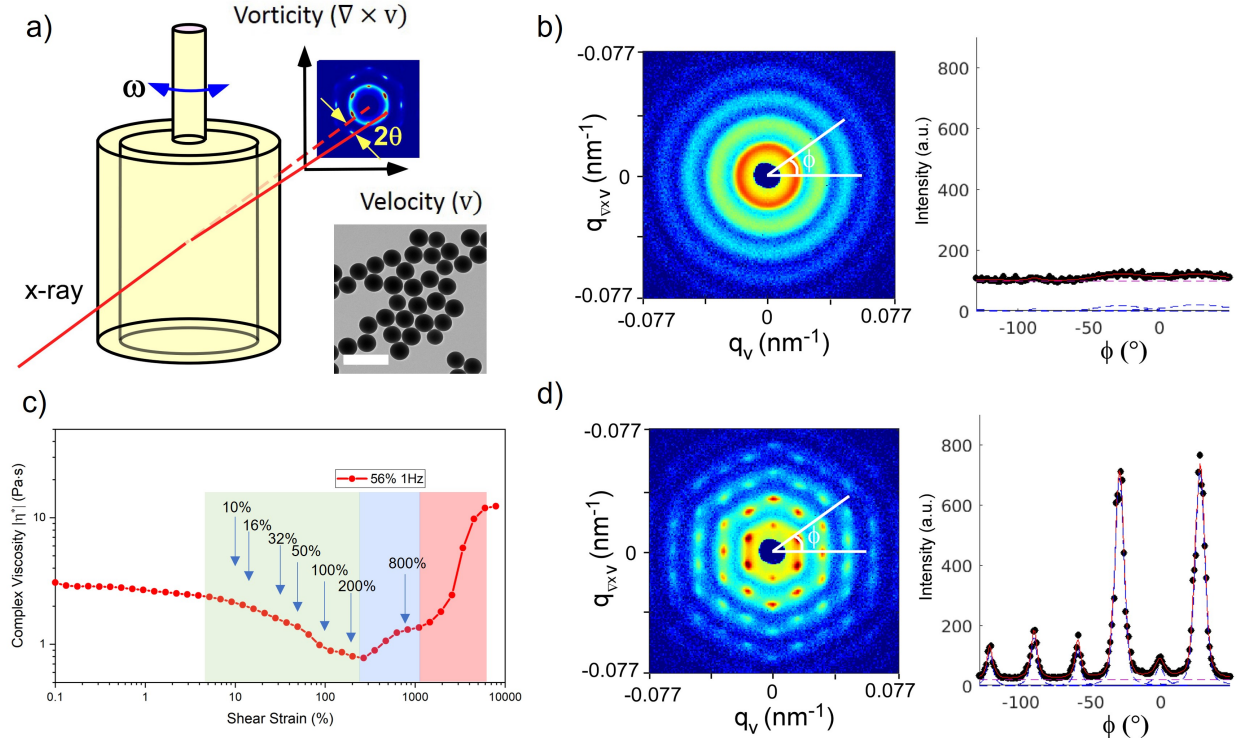


Figure 1: (a) Schematic of the *in situ* SAXS setup. The lower-right inset is a TEM image of our colloidal silica sample. Scale bar is  $1 \mu\text{m}$ . (b) Scattering pattern in the velocity-vorticity plane from a quiescent sample after sonication to remove any crystallites. (c) The magnitude of the complex viscosity vs. oscillatory shear strain amplitude under a strain sweep measurement,  $f = 1\text{Hz}$ . Green region indicate a shear thinning region corresponding to shear induced ordering, the blue region indicate a shear thickening region related to shear induced order-to disorder transition and the red region indicate shear thickening driven by hydrodynamic effect and/or friction between particles. (d) Scattering pattern of the sample when it reaches 100% shear strain amplitude. Dots in the right panels in (b) and (c) shows the experimental data of integrated scattering intensity vs. azimuthal angle  $\phi$ . Lines in the panels are fitting curves as described in the text.

crystals and the kinetics of shear-induced melting can be extremely important, not only for developing a deeper understanding of the behavior of complex fluid, but it can also have a direct technological impact as shear induce ordering has already been used in industry to manufacture unique optical devices.<sup>18,19</sup> However, very few studies have focused on this aspect, largely because most experimental techniques lack the time resolution and penetration depth to probe the internal structural evolution in a dense colloid. Here, using a time-dependent Rheology-Small angle x-ray scattering (Rheo-SAXS) instrument, we exam-

ine the kinetics of crystallization during oscillatory shear in a dense colloidal solution with a high temporal resolution. We show that the macroscopic rheological response has a strong correlation with the local structural ordering, even though under certain conditions, there is a strong fluctuation in local structural ordering. Measurements within a single oscillatory cycle also show, in the intermediate region where the system is partially ordered, the degree of ordering is phase dependent. The degree of ordering is highest when the strain amplitude is at its maximum and lowest when the strain rate is the highest.

## 2 Materials and Methods

**Sample Preparation** The system we studied consisted of relatively monodispersed silica colloids ( $\sim 390\text{nm}$ ) synthesized using the Stöber method. Typical synthesis involved combining 32mL of ultra-pure distilled water (Fisher Scientific), 221mL anhydrogus ethanol (Fisher Scientific) and 59mL 30-33% ammonium hydroxide solution (Sigma-Aldrich) and heating the mixture to  $50^\circ\text{C}$ . 17mL of tetraethyl orthosilicate (TEOS) from Sigma-Aldrich was injected rapidly into the stirring mixture. The solution turned whitish cloudy after a few minutes. The reaction was allowed to continue for 2 hours, followed by adding 7mL of 3-trimethoxysilyl propyl methacrylate (TMSPM)(Chem-Impex Int'l). The reaction was allow to proceed for another 45 minutes. TMSPM coating removes the surface charge on the as-prepared silica particles, and the molecular length is short enough that the coated particles can still be treated as hard spheres. The as-prepared silica nanoparticles was centrifuged and washed with ethanol three times, and finally dried in vacuum overnight. We use polyethylene glycol (M.W. 200g/mol)(PEG-200) as a solvent, because PEG-200 is less likely to evaporate during the course of our experiment. TMSPM functionalization also enable silica particles to be well-dispersed in PEG-200. We mainly focus on a particle volume fraction of 56%, which is determined by weighing the solid mass of silica particles and then convert it into particle volume using an experimentally determined silica density of 1.865g/mL. The detailed exper-

imental protocol to determine the density of silica particle was published earlier by Lee et al.<sup>20</sup> and Maranzano et al.,<sup>21</sup> and our analysis is included in Figure S1 of the supporting materials. We note that the density of silica nanoparticle obtained in our synthesis is much lower than fuse silica density of  $2.2g/cm^3$  and crystalline quartz density of  $2.65g/cm^3$ . But this is consistent with earlier report that Stöber synthesis yield much porous silica structure.<sup>22</sup> A suitable amount of PEG-200 solvent was added to make a 56% dispersion, assuming the total volume of the two components was additive. The sample was sonicated and vortex stirred repeated until a homogeneous and optically transparent sample is obtained.

**Rheo-SAXS Setup** The combined setup was constructed at 8ID-I of the Advanced Photon Source, Argonne National Lab. A collimated x-ray beam (11 keV,  $15\ \mu\text{m}$  in width and height) passes through the center of the cylindrical polycarbonate Couette cell in the horizontal plane, perpendicular to the vertical rotational axis of the rheometer. Figure 1a is the schematic of the experimental geometry. The shear cell is controlled by a Anton Paar MCR 301 Rheometer, and has an inner wall diameter of 11.4mm, and the diameter of the bob is 11.0mm. The x-ray beam traverses along with the shear gradient direction and the scattering pattern is collected in the velocity-vorticity plane using a 2D pixel array detector with  $q$  being the scattering wavevector with the value of  $q = 2k \sin \theta$ , where  $k = 2\pi/\lambda$  is the wavevector and  $2\theta$  is the scattering angle. Experimental trigger is programmed to allow synchronization of x-ray scattering data collection and rheology data collection.

### 3 Results and Discussion

For 56% volume fraction, the equilibrium structure of a hard sphere colloid is in the crystalline regime. Therefore, the sample was subjected to a vigorous sonication to remove any possible crystallites already existing in the sample, until an amorphous scattering ring was confirmed using small angle x-ray scattering (SAXS). (Figure 1b). Crystallization would gradually occur if we leave the sample in this state undisturbed, but over a time frame much

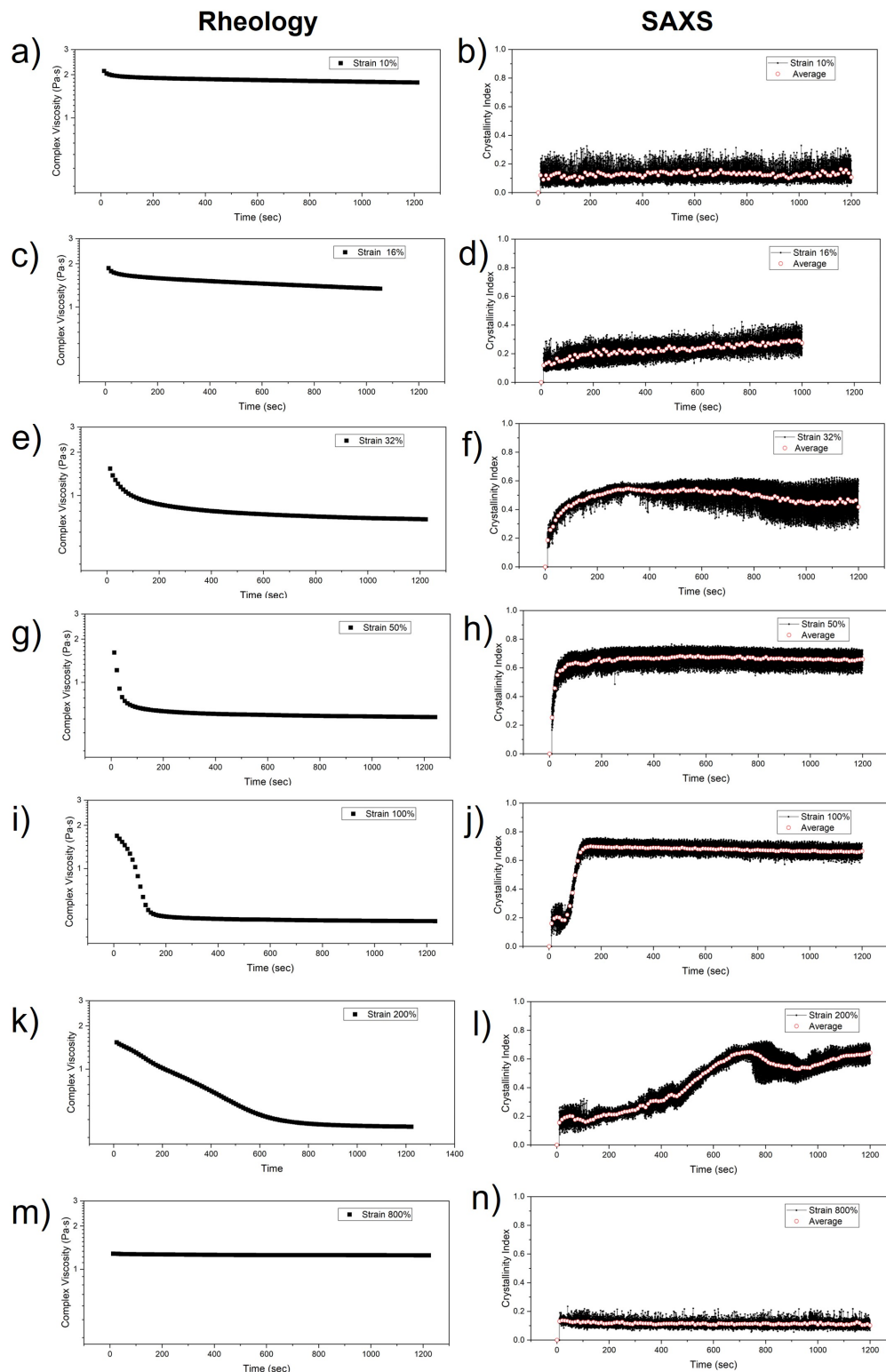


Figure 2: Time dependence of complex viscosity magnitude ( $|\eta^*|$ ) and crystalline index (CI) parameter during an oscillatory shear (1Hz) with strain amplitude at (a-b) 10%, (c-d) 16%, (e-f) 32%, (g-h) 50%, (i-j) 100%, (k-l) 200%, (m-n) 800%. SAXS data (dark point) were collected at 10Hz, and each frame's CI were analyzed using the method outlined in the text. Open circles in CI plots are the average of the data to serve as a guide to eye. The data in panel (c-d) is slightly shorter due to an unexpected loss of x-ray beam during the experiment.

longer than our experimental time. However, we found that a moderate shear can induce ordered structure formation much more rapidly, particularly with an oscillatory shear.<sup>6,13,23</sup> Our previous experiments have shown that, with further increase of strain amplitude, oscillatory shear is likely to induce an order-to-disorder transition that destroys the crystals formed in the system.<sup>12</sup> Figure 1c shows the magnitude of complex viscosity plotted against strain amplitude at 1Hz. Corresponding data in the form of elastic modulus and loss modulus are shown in Figure S2 of the supporting materials. As we increase the strain amplitude, the viscosity continues to decrease, which is associated with a gradual formation of ordered layer structure (Green region in Figure 1c). In this ordered state, particles are driven to form layers perpendicular to the shear gradient direction. Within each layer, hexagonal ordering of particles appears. However, unlike face-centered cubic (fcc) or hexagonal close-packed (hcp) structures, there is no clear registry of particles between the layers. Adjacent layers of particles can slide relative to each other along the grooves in the hexagonal lattice, which significantly reduce the friction between layers in comparison with the case that adjacent layers of particles are highly disordered.<sup>6</sup> A trademark of this so-called sliding layer structure is the scattering intensity along the vorticity direction is relatively weak compared with the other two directions (Figure 1d), as observed previously in light scattering experiment,<sup>6</sup> neutron scattering<sup>24</sup> and simulation.<sup>13</sup> After 100-200% strain, the complex viscosity increases again associated with melting of the crystalline layers (Blue region in Figure 1c). In this disordered particle arrangement, particle relative motion can be hindered locally, and create a high viscosity state. Above a very high shear strain (1200%), there is an additional shear thickening step (Red region in Figure 1c), which is associated with either hydrodynamic effect and/or frictional forces between the particles. At highest strain amplitudes (>8000%), elastic modulus decreases with the strain amplitude and loss modulus reaches a plateau, this could be an indication that wall slip may play a role in this regime (Figure S2). We also note that, at large oscillatory shear strain, the system could enter a regime that stress response might have non-sinusoidal components. In that case, a simple picture of using storage module ( $G'$ ), loss

module ( $G''$ ) and complex viscosity  $|\eta^*|$  is no longer valid strictly speaking, and several more complex approaches have been developed over the years to analyze the data.<sup>25-28</sup> However, since our current focus is to examine the relationship between rheology and microstructure, we adopted an approach to use sinusoidal response as a way to simplify the rheology response of the system.

The degree of ordering under various oscillatory conditions can be quantified by integrating the scattering intensity radially up to the third order diffraction peaks, and then plotting the integrated intensity against the azimuthal angle  $\phi$ , as shown in Figure 1b and 1d. Typically, the scattering intensity plot will consist of an angular independent component that is associated with the disordered portion of the sample and an angular dependent component that comes from the crystalline components. By de-convoluting the total intensity ( $I_{total}$ ) into these two components,  $I_{crystalline}$  and  $I_{amorphous}$ , we can define a crystalline index (CI) parameter as  $CI = I_{crystalline}/I_{total}$ , which is an indicator of the degree of ordering within the sliding layer.<sup>12</sup>

Strain sweep measurements in Figure 1c was carried out continuously while collecting data at each oscillatory strain for only ten seconds. It is likely that the system has not reached its steady state under each oscillatory condition. Therefore, we decided to carry out a more detailed time-dependent study at several oscillatory shear strains (with specific amplitude indicated in Figure 1c). Figure 2 shows the comparison of rheology data (complex viscosity vs. time) and the simultaneous SAXS measurement (CI vs. time). Corresponding rheological data plotted in elastic modulus and loss modulus are shown in Figure S3 in the supporting document. The SAXS data were collected at a rate of 10 frames per cycle of oscillation, and each scattering image frame was analyzed using the method outline above to obtain the CI value. We also show an average of these data points (open circles) to guide the eye. Each rheology data point was averaged over a time period of 10s in order to improve the statistics of the data.

A key takeaway of Figure 2 is that the macroscopic rheology data present more or less

the same trend as the local structure changes measured by SAXS. For strain amplitude at 10%, there is very little change of ordering, and the change in complex viscosity ( $|\eta^*|$ ) is also very small. At 16% strain, there is a small degree of ordering which increases slowly with time in conjunction with a slow decrease of viscosity. For 32% and 50%, a relative significant amount of ordering quickly develops in the system and the same monotonic change in the viscosity is also observed. However, for 100% strain, there is a small plateau in the CI curve at the early stage of the shear, possibly caused by a burst of crystallites forming during this stage. These crystallites are stable for a period of time before they start to grow. This is also reflected in the rheology data, in which the early decrease of viscosity  $|\eta^*|$  consists of two different stages with the first stage decreasing much slower than the second one. At 200% strain, both the  $|\eta^*|$  and CI change over 600-700s, a much longer time scale to reach a dynamic equilibrium than any other shear conditions. Non-monotonic change of CI is also a very distinct feature under this condition, indicating that the development of local structure ordering is not trivial, driven by competing effects that induces the ordering (shear) and disrupts the ordering (hydrodynamic effect). At 800% strain, both  $|\eta^*|$  and local ordering remain unchanged within the time frame of the experiment. These kinetics data show a high fidelity between the macroscopic rheological response and the local structure ordering.

Fitting the rheology data shows that, in the case of low shear strains, the experimental kinetics can be described by two different exponential functions, or one exponential and one linear term (linear term can also come from an approximation when one exponential time constant is much longer than the experimental measurement time) (see Figure S4 in the supporting information). This is reminiscent of the kinetics in a solvent evaporation induced 2D nanoparticle crystal formation on a liquid-air interface,<sup>29</sup> albeit under a very different circumstance. In the case of evaporation induced 2D crystals, nanocrystals can be incorporated directly into the growing crystal domain from below or added to the perimeter of the domain through diffusion. Depending upon the flux added to the liquid-air interface, particle diffusion length along the interface and the size of growing domains relative to the

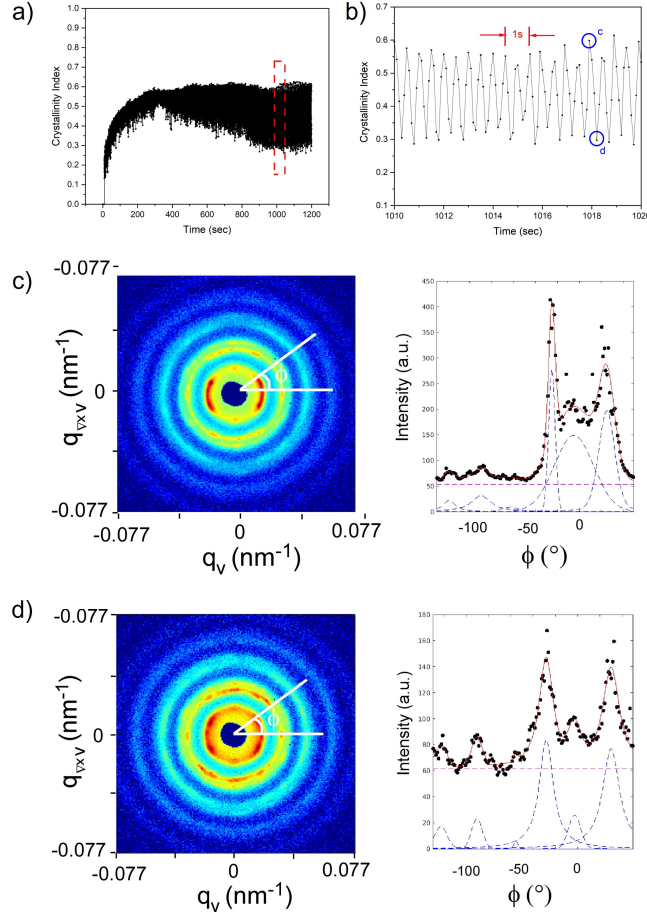


Figure 3: The crystalline ordering parameter (CI) during an oscillatory shear (1Hz) with strain amplitude at (a) 32%, (b) a zoomed-in region outlined in panel (a). Scattering pattern and integrated intensity vs. azimuthal angle when the oscillatory shear is at its maximum amplitude (point c in panel b) (c) and when the strain rate is at its maximum (point d in panel b) (d). In (c-d), solid scattered data is the experimental integrated intensity, purple dashed lines are fitting curves for the crystalline component, red dashed lines are fitting curves for the amorphous component, and solid red line are the total fitting intensity.

Voronoi cell radius changes, and consequently both linear kinetics and exponential kinetics have been observed. In the shear induced crystal formation, similar underlying mechanism could control the kinetics, although parameters such as diffusion length and Voronoi cell dimension may be modified by different shear conditions.

Since SAXS data were collected at a much higher frequency (10 Hz) relative to the oscillatory shear frequency (1Hz), this allows us to detect the local structure change within a single oscillatory cycle. Figure 3 (a-b) shows a zoomed in area of CI plot for 32% strain.

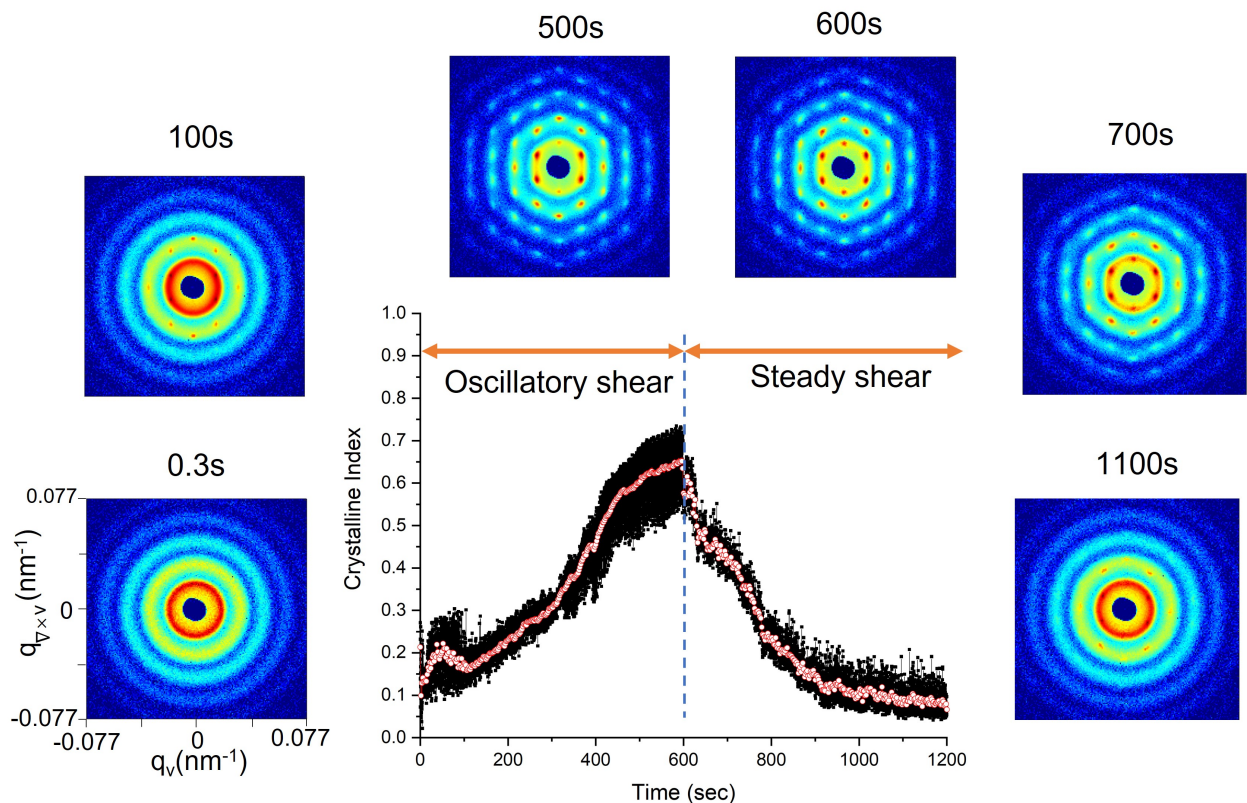


Figure 4: Steady shear at  $0.1s^{-1}$  melt the crystals formed after an oscillatory shear (1Hz) at the strain amplitude at 200% for 600s. Inset shows the scattering pattern of the sample at different stage of the shear.

With this intermediate strain, the degree of ordering changes dramatically at a frequency of 2Hz, twice the frequency that has been applied. This means that, within a single sinusoidal strain cycle, the structure oscillates between two different metastable structures (see movie in the supporting information). Since our rheology data were collected at a much slower rate (10s per data point) than the x-ray data (0.1s per data point), we can not determined precisely whether is a phase shift between the instantaneous strain deformation and the crystalline index. However, the fact that crystalline index oscillates at twice the frequency as the strain deformation, and considering the symmetry of the system, it is clear that the degree of ordering is highest when the strain amplitude is at its maximum (Figure 3c) and reaches the most disordered state when the strain amplitude is zero (Figure 3d). This phase dependent ordering during oscillatory shear has not been observed previously.

To study the stability of shear induced crystals, we use oscillatory shear at 200% strain amplitude for 600s to establish a high degree of crystallinity inside the shear cell (Figure 4, oscillatory shear segment). At this point, we set the stress in the rheometer to zero. We observed the sliding layer structure would relax into hcp/fcc crystals very quickly, with scattering intensity along the vorticity direction becoming nearly as intense as the other two directions. The crystal structure would remain in place for a long time if it is left undisturbed, at least for 12 hours as observed in our study (See Figure S5 in the supporting information), which indicates the ordered structure is extremely stable. However, when the crystals are subjected to a steady shear, even with a small shear rate of  $0.1s^{-1}$ , it would undergo a shear induced melting (Figure 4, steady shear segment). Corresponding changes in the viscosity during these two segments can be found in the Figure S6 of the supporting materials. The shear melting process is initiated through crystallites losing orientational ordering first (as indicated by a broadening of the first order scattering peak along the azimuthal directions (Figure 4, 700s), followed by a gradual breakdown of their translational ordering (Scattering intensity broadens along the q direction, as shown in Figure 4, 1100s). For shear rate at  $0.1s^{-1}$ , there are still some small amount of crystallites remaining after 1200s of continuous shear. An increase of the shear rate will speed up the kinetics of shear induced melting and remove the remaining crystallites more thoroughly. Data using shear rate at  $0.5s^{-1}$  and  $1s^{-1}$  are included in the Figure S6 of the supporting materials. Also noted is that, in all three cases, during oscillatory shear segments, the system evolves toward a highly ordered state through different kinetic pathways, which is consistent with non-monotonic kinetics observed in Figure 2l. This indicates the local ordering of particles is still highly heterogenous and non-monotonic, driven by the competition between shear induced ordering and hydrodynamic effects that could disrupt the ordering.

The fact that an oscillatory shear with a strain amplitude 100% – 200% is more likely to induce crystal formation, whereas a steady shear or a high amplitude oscillatory shear can bypass or melt the crystals is likely related to the spatial heterogeneity of the local potential

landscape. With oscillatory shear, each particle simply has more opportunities to explore the local energy landscape, and find a more thermodynamically favored state, which is a crystal phase at a volume fraction of 56%. A recent molecular dynamics simulation study found that steady shear can induce ordered crystal formation directly.<sup>30</sup> However, the simulation was conducted using particles without any friction between them. In real samples, friction between particles is almost inevitable, which means particle rearrangements are much more difficult. Oscillatory shear simply explores more structural rearrangement possibilities and can therefore more easily facilitates the transition of particles into an ordered state.

## 4 Conclusion

In summary, our high temporal resolution Rheo-SAXS measurements show that the local structural ordering is highly correlated with the rheological response of the entire sample. Oscillatory strain amplitude is a key parameter that controls the degree of the ordering and the kinetic pathway towards a dynamic equilibrium. Of particular interest is the finding that the local structural evolution can be nonmonotonic, especially when shear induced ordering is in competition with hydrodynamic force driven shear melting (i.e. 200%). Furthermore, within a single cycle of oscillatory shear, the local structure is phase dependent, dynamically oscillating between two metastable states. These findings offer new insight into the interaction between particles in a dense colloid.

**Author Contributions:** S. Narayanan and X. M. Lin designed the experiment, J. Lee conducted the initial experiment. Q. He, J. Dinic, W. Chen conducted additional experiments, H. He, S. Narayanan and X. M. Lin did the data analysis and contributed to the writing of the manuscript.

## Acknowledgement

The authors thanks for many fruitful discussions with James Horwath, Qingteng Zhang, Eric Dufresne, Subramanian Sankaranarayanan and Emanuela Del Gado. Work performed at the Center for Nanoscale Materials and Advanced Photon Source, both U.S. Department of Energy Office of Science User Facilities, was supported by the U.S. DOE, Office of Basic Energy Sciences, under Contract No. DE-AC02-06CH11357. The work is also partially supported by the LDRD program of Argonne National Laboratory. Work by Hongrui He was partially supported by the Advanced Materials for Energy-Water Systems (AMEWS), an Energy Frontier Research Center funded by the U.S. Department of Energy, Office of Science, Basic Energy Sciences. Work by Qiming He, Jelena Dinic, Wei Chen was supported by the U.S. Department of Energy, Office of Science, Office of Basic Energy Sciences, Materials Science and Engineering Division.

## Supporting Information Available

The Supporting Information is available free of charge at <https://www>.

- Determination of silica nanoparticle density
- Rheological data on oscillatory shear strain sweep.
- Rheology data during oscillatory shear at different strain amplitudes.
- Kinetics of Rheology during oscillatory shear at different strain amplitudes.
- Stability of Oscillatory Shear induced Crystal
- Steady Shear induced Melting of Crystals formed during oscillatory shear.
- Movie on the dynamic oscillation between two different states at 32% shear strain.

## References

- (1) Vermant, J.; Solomon, M. J. Flow-induced structure in colloidal suspensions. *Journal of Physics: Condensed Matter* **2005**, *17*, R187–R216.
- (2) Poon, W.; Haw, M. Mesoscopic structure formation in colloidal aggregation and gelation. *Advances in Colloid and Interface Science* **1997**, *73*, 71–126.
- (3) Pusey, P.; van Megen, W. Phase behaviour of concentrated suspensions of nearly hard colloidal spheres. *Nature* **1986**, 340–342.
- (4) Richard, D.; Speck, T. The role of shear in crystallization kinetics: From suppression to enhancement. *Scientific Reports* **2015**, *5*, 14610–14616.
- (5) Hoffman, R. L. Discontinuous and Dilatant Viscosity Behavior in Concentrated Suspensions. I. Observation of a Flow Instability. *Transactions of the Society of Rheology* **1972**, *16*, 155–173.
- (6) Ackerson, B. J.; Pusey, P. N. Shear-Induced Order in Suspensions of Hard Spheres. *Phys. Rev. Lett.* **1988**, *61*, 1033–1036.
- (7) Clark, N. A.; Hurd, A. J.; Ackerson, B. J. Single Colloidal Crystals. *Nature* **1979**, *281*, 57–60.
- (8) Haw, M. D.; Poon, W. C. K.; Pusey, P. N. Direct observation of oscillatory-shear-induced order in colloidal suspensions. *Physical Review E* **1998**, *57*, 6859–6864.
- (9) Phung, T. N.; Brady, J. F.; Bossis, G. Stokesian Dynamics simulation of Brownian suspensions. *Journal of Fluid Mechanics* **1996**, *313*, 181–207.
- (10) Kulkarni, S. D.; Morris, J. F. Ordering transition and structural evolution under shear in Brownian suspensions. *Journal of Rheology* **2009**, *53*, 417–439.

- (11) Xu, X.; Rice, S. A.; Dinner, A. R. Relation between ordering and shear thinning in colloidal suspensions. *Proceedings of the National Academy of Sciences* **2013**, *110*, 3771–3776.
- (12) Lee, J.; Jiang, Z.; Wang, J.; Sandy, A. R.; Narayanan, S.; Lin, X.-M. Unraveling the Role of Order-to-Disorder Transition in Shear Thickening Suspensions. *Physical Review Letters* **2018**, *120*, 028002.
- (13) Besseling, T. H.; Hermes, M.; Fortini, A.; Dijkstra, M.; Imhof, A.; van Blaaderen, A. Oscillatory shear-induced 3D crystalline order in colloidal hard-sphere fluids. *Soft Matter* **2012**, *8*, 6931–6939.
- (14) Koumakis, N.; Brady, J. F.; Petekidis, G. Amorphous and ordered states of concentrated hard spheres under oscillatory shear. **2016**, *233*, 119–132.
- (15) Wu, Y. L.; Derks, D.; van Blaaderen, A.; Imhof, A. Melting and crystallization of colloidal hard-sphere suspensions under shear. *106*, 10564–10569.
- (16) Hoffman, R. L. Explanations for the cause of shear thickening in concentrated colloidal suspensions. *Journal of Rheology* **1998**, *42*, 111–123.
- (17) Brown, E.; Jaeger, H. M. Shear thickening in concentrated suspensions: phenomenology, mechanisms and relations to jamming. *Reports on Progress in Physics* **2014**, *77*, 046602.
- (18) Li, Y.; Fan, Q.; Wang, X.; Liu, G.; Chai, L.; Zhou, L.; Shao, J.; Yin, Y. Structural Coloration: Shear-Induced Assembly of Liquid Colloidal Crystals for Large-Scale Structural Coloration of Textiles (Adv. Funct. Mater. 19/2021). *Advanced Functional Materials* **2021**, *31*, 2170133.
- (19) Snoswell, D. R.; Kontogeorgos, A.; Baumberg, J. J.; Lord, T. D.; Mackley, M. R.; Spahn, P.; Hellmann, G. P. Shear Ordering in Polymer Photonic Crystals. Conference on Lasers and Electro-Optics 2010. 2010; p CThS5.

- (20) Lee, Y. S.; Wagner, N. J. Rheological Properties and Small-Angle Neutron Scattering of a Shear Thickening, Nanoparticle Dispersion at High Shear Rates. **2006**, *45*, 7015–7024.
- (21) Maranzano, B. J.; Wagner, N. J. The effects of particle size on reversible shear thickening of concentrated colloidal dispersions. *The Journal of Chemical Physics* **2001**, *114*, 10514–10527.
- (22) Parnell, S. R.; Washington, A. L.; Parnell, A. J.; Walsh, A.; Dalgliesh, R. M.; Li, F.; Hamilton, W. A.; Prevost, S.; Fairclough, J. P. A.; Pynn, R. Porosity of silica Stöber particles determined by spin-echo small angle neutron scattering. **2016**, *12*, 4709–4714.
- (23) Yan, Y.; Dhont, J.; Smits, C.; Lekkerkerker, H. Oscillatory-shear-induced order in nonaqueous dispersions of charged colloidal spheres. *Physica A: Statistical Mechanics and its Applications* **1994**, *202*, 68–80.
- (24) Chen, L. B.; Ackerson, B. J.; Zukoski, C. F. Rheological consequences of microstructural transitions in colloidal crystals. **1994**, *38*, 193–216.
- (25) Wilhelm, M. Fourier-Transform Rheology. *Macromolecular Materials and Engineering* **2002**, *287*, 83–105.
- (26) Cho, K. S.; Hyun, K.; Ahn, K. H.; Lee, S. J. A geometrical interpretation of large amplitude oscillatory shear response. *Journal of Rheology* **2005**, *49*, 747–758.
- (27) Klein, C. O.; Spiess, H. W.; Calin, A.; Balan, C.; Wilhelm, M. Separation of the Nonlinear Oscillatory Response into a Superposition of Linear, Strain Hardening, Strain Softening, and Wall Slip Response. *Macromolecules* **2007**, *40*, 4250–4259.
- (28) Donley, G. J.; de Bruyn, J. R.; McKinley, G. H.; Rogers, S. A. Time-resolved dynamics of the yielding transition in soft materials. *Journal of Non-Newtonian Fluid Mechanics* **2019**, *264*, 117–134.

- (29) Bigioni, T. P.; Lin, X.-M.; Nguyen, T. T.; Corwin, E. I.; Witten, T. A.; Jaeger, H. M. Kinetically driven self assembly of highly ordered nanoparticle monolayers. *Nature Materials* **2006**, *5*, 265–270.
- (30) Goyal, A.; Del Gado, E.; Jones, S. Z.; Martys, N. S. Ordered domains in sheared dense suspensions: The link to viscosity and the disruptive effect of friction. *Journal of Rheology* **2022**, *66*, 1055–1065.

# TOC Graphic

